Proceedings of the Sixth International Conference on
Railway Technology: Research, Development and Maintenance
Edited by: J. Pombo
Civil-Comp Conferences, Volume 7, Paper 2.8
Civil-Comp Press, Edinburgh, United Kingdom, 2024
ISSN: 2753-3239, doi: 10.4203/ccc.7.2.8

Train Running Safety on Bridges: Methodologies and Applications

P. A. Montenegro

CONSTRUCT-LESE, Faculty of Engineering, University of Porto
Porto, Portugal

Abstract

Train running safety is a major concern among railway engineers, since a derailment may cause significant personal and material damages. Such issue becomes particularly worrying if the derailment occurs on bridges, especially at high-speeds, where the consequences may be even worse. The development of large high speed (HS) railway networks around the globe characterized by strict design requirements led to the construction of lines with more than 75% of their extension built viaducts and bridges. Consequently, the probability of a high-speed train derail over a bridge during the occurrence of hazards that might jeopardize its safety increases substantially. The present paper is, therefore, a summary of the work performed by the author in the last years about the methodologies and applications on the analysis of the stability of trains when subjected to external actions, such as crosswinds or earthquake. This work also addresses future challenges regarding the studies that still have to be carried out to go from the explicit, but time-consuming, derailment analysis with train-track-bridge interaction models to more simple methods that may be adopted in codes and standards to be adopted by bridge design engineers in a daily basis.

Keywords: train running safety, railway bridges, train-track-bridge interaction, derailment, wind, earthquake.

1 Introduction

In more recent years, the running safety of train moving over bridges have been becoming an important issue in the railway engineering. The necessity to fulfil the

strict design requirements of HS railways led to a high percentage of viaducts and bridges in the lines intended to this type of traffic. Some countries in Asia, such as China and Japan, for example, have a highly developed HS railway network in which some of the lines have more than 75 % of bridges and viaducts [1].

Derailments may be a consequence of several factors that have been studied in the past but are being treated with more accuracy in the last few years due to the increment in the computational efficiency to perform complex numerical train-structure interaction analyses. Among these factors it is important to highlight those related to poor track quality caused by lack of maintenance [2]; existence of isolated defects in the rail [3]; occurrence of pier collisions [4] or settlements [5]; issues in the vehicle itself, namely defects on the gears (bogies or wheelsets) or in the wheels [6]; or natural hazards, such as earthquakes [7,8,9], crosswinds [10,11,12,13] or snow [14].

To accurately assess the train running safety or the derailment phenomenon on bridges, it necessary to develop complex and robust vehicle-structure interaction models which are able to capture the dynamic behaviour of the coupling system and to compute the contact forces that arise in the wheel-rail interface. These models are only available in a few multibody simulation (MBS) commercial software, but with important limitations regarding the structural modelling, since they are limited to simple models of flexible tracks and cannot reproduce the complexity of a bridge structure. On the other hand, the generic commercial Finite Element Method (FEM) packages, which are capable of modelling structures with any degree of complexity, do not have specific train-track-bridge interaction (TTBI) coupling methods incorporated. Therefore, when the objective is to analyse the interaction between the train and a complex flexible structure, such as a bridge or viaduct, commercial softwares are not very convenient, efficient and elaborate for this intent so far. This limitation led to the development of design criteria based on indirect indicators related to the response of the bridge in order to allow bridge designers to easily and implicitly assess the train running safety. However, with the exception of the Japanese standard [15], which takes into consideration the earthquake action, the majority of the criteria do not take into consideration different scenarios other than those representing the regular operation. Hence, to explicitly assess the traffic safety based on actual safety criteria that take into consideration the behaviour of the wheel-rail interface, researchers have been developing TTBI models able to accurately evaluate the train stability under different conditions, such as the presence of crosswinds, earthquakes or other hazards (see Figure 1).

According to Montenegro et al. [1], The train running safety on bridges may be assessed through the two following approaches, which are illustrated in Figure 1: i) through indirect indicators related to the bridge response, referred here as the normative approach; and ii) through the evaluation of running safety criteria obtained from dynamic TTBI analysis, designated hereinafter as explicit approach. While the former is easily implemented, the latter is more accurate and allows the consideration of any kind of scenario with any type of sources of excitation. Hence, for the normative approach, the bridge model and train loads are generally sufficient to assess the running safety, since the bridge indicators may be calculated with simple static or dynamic analyses. On the other hand, for the explicit approach, a full TTBI model is required to obtain the contact forces and, consequently, the safety indexes.

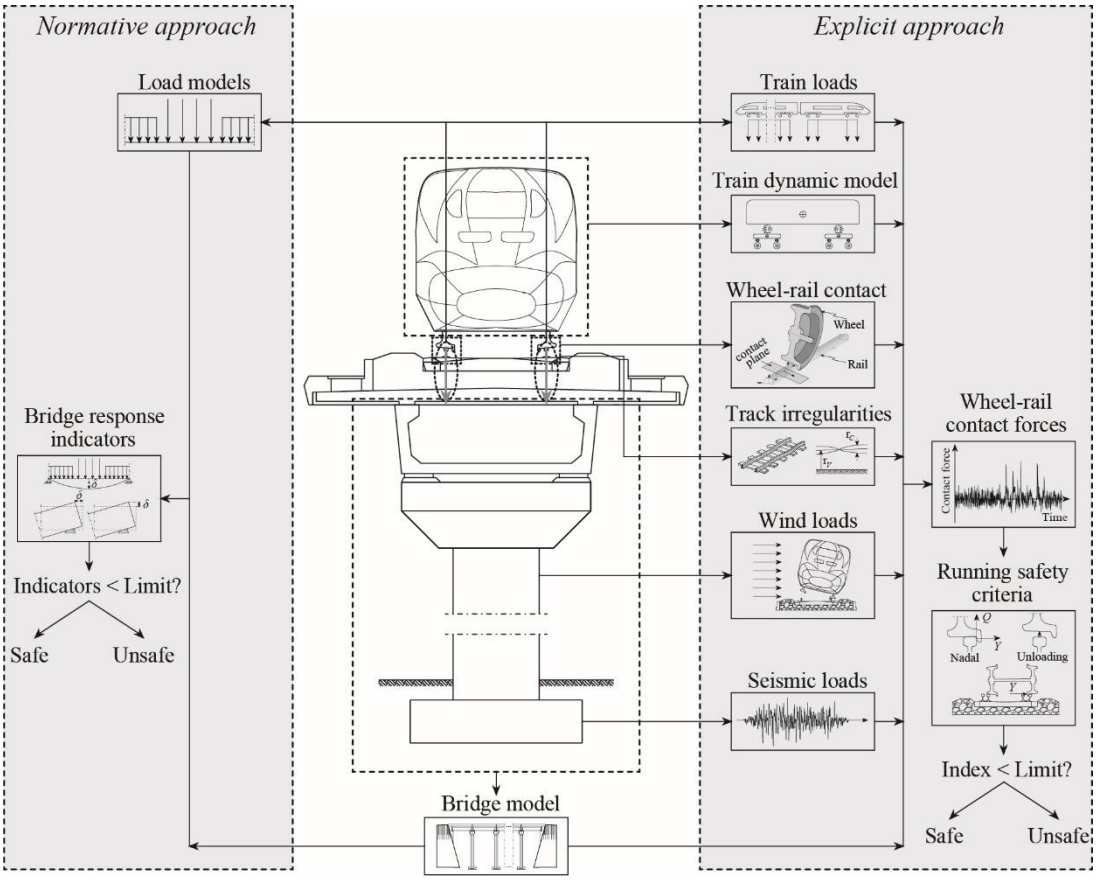

Figure 1: Normative and explicit approaches to evaluate the train running safety over bridges.

The present paper aims to present an overview of the author's work performed in the last years about the methodologies and applications on the analysis of the stability of trains when subjected to external actions, such as crosswinds or earthquake. In the end, this work also addresses the challenges that need to be overcome in the future to improve the current criteria stipulated in the standards, in particular those presented in the Eurocodes [16,17], related with train running safety on bridges

2 TTBI methodology to assess train running safety

2.1. TTBI model presentation

The TTBI models available in the literature may be classified according to the method used to make the compatibility between the two interacting sub-systems, i.e., coupled or uncoupled methods (an extensive literature review can be found in [18]). The results presented here were obtained through a TTBI coupled model developed and validated in [19,20,21]. A brief presentation of the TTBI model is presented next.

In the present method, the governing equilibrium equations of the vehicle and structure are complemented with additional constraint equations that relate the displacements of the contact nodes of the vehicle with the corresponding nodal displacements of the structure. The formulation has been developed by [20] and takes

into account the geometry of the wheel and rail and the behaviour of the contact interface. The train-structure problem can be expressed in a matrix form as

$$\begin{bmatrix} \bar{\mathbf{K}} & \bar{\mathbf{D}} \\ \bar{\mathbf{H}} & \mathbf{0} \end{bmatrix} \begin{bmatrix} \Delta \mathbf{a}_F^{i+1} \\ \Delta \mathbf{X}^{i+1} \end{bmatrix} = \begin{bmatrix} \boldsymbol{\psi}\left(\mathbf{a}^{t+\Delta t,i}, \mathbf{X}^{t+\Delta t,i}\right) \\ \bar{\mathbf{r}} \end{bmatrix} \tag{1}$$

where $\bar{\mathbf{K}}$ is the current effective stiffness matrix of the vehicle-structure system, $\bar{\mathbf{D}}$ is a matrix that relates the contact forces, defined with respect to the target element coordinate system, with the nodal forces defined in the global coordinate system, $\bar{\mathbf{H}}$ is the transformation matrix that relates the nodal displacements of the target elements, defined in the global coordinate system, with the displacements of the auxiliary points defined with respect to the target element coordinate system, $\boldsymbol{\psi}$ is the residual force vector that depends on the nodal displacements $\mathbf{a}$ and on the contact forces $\mathbf{X}$ and $\bar{\mathbf{r}}$ the vector with the irregularities that may exist in the contact interface. The superscript $t+\Delta t$ indicates the current time step, while i and $i+1$ denotes the previous and current Newton iteration, respectively.

Regarding the wheel-rail contact model, the nonlinear Hertz contact theory [27] is used to analyze the normal contact problem, in which the normal contact force *Fn* (see Figure 3) between the wheel and rail is given by [28]

$$F_n = K_h \, d^{\frac{3}{2}} \tag{2}$$

where d is the penetration and K_h is a generalized stiffness coefficient that depends on the material properties of the bodies in contact, such as the Young modulus and the Poisson ratio, and the curvatures of the surfaces at the contact point. As for the tangential creep forces in the longitudinal, F_ξ, and lateral , F_η, directions (see Figure 3), these are precalculated and stored in a lookup table, based on the USETAB algorithm [22], to be later interpolated during the dynamic analysis as a function of the creepages and the semi-axes ratio of the contact ellipse.

2.2. Running safety criteria

The explicit assessment of the derailment risk is carried out through three safety criteria, namely Nadal, Prud'homme and unloading, based on the wheel-rail contact forces. Table 1 presents the indexes ξ associated to each of the aforementioned criteria, together with their safety limits and the filters stipulated by the norms to be applied to their time-histories.

Criterion	Criterion index	Allowances	Filter type
Nadal (each wheel)	$\xi_N = \frac{Y}{Q}$	0.8	Low-pass filter with cut-off frequency of 20 Hz and a 4th order filter after a sliding mean based on a window size of 2.0 m [23].
Prud'homme (each wheelset)	$\xi_P = \frac{\sum_{ws} Y}{10 + \frac{2Q_0}{3}\,[\text{kN}]}$	1.0	
Unloading (each side of each bogie)	$\xi_U = 1 - \frac{Q_i + Q_j}{2Q_0}$	0.9	Low-pass filter with a cut-off frequency of 2 Hz using a 4th order Butterworth filter [24].

Q_0: static vertical wheel load.

Q: vertical wheel contact force.

$Q_{i,j}$: vertical contact force on wheels i and j from the same side of the bogie.

Y: lateral wheel contact force.

$\sum_{ws} Y$: total lateral contact force exerted by a single wheelset.

Table 1: Safety criteria used in the present study to assess the train running safety.

3 Case study – running safety against earthquakes

3.1. Case study presentation

The first case study presented in this work consisted of the running safety analysis of a HS train running over the Alverca viaduct, in Portugal, subjected to moderate earthquakes. This is an important point to take into consideration, since the running safety of trains might be jeopardized not only by intense shakings, but also by moderate earthquakes, which may not cause significant damage to the structure.

The Alverca viaduct is located in Portugal and its structure comprises several simply supported spans with 21 m length. The deck consists of a prefabricated and prestressed U-shaped beam on which pre-slabs serving as formwork to the concrete upper slab cast *in situ* are placed, forming a single-cell box girder deck. The numerical model of the viaduct is developed in ANSYS® [25]. The deck, piers, sleepers and rails are modelled using beam finite elements, while the bearing supports, ballast and pads are modelled using linear spring-dampers. Mass point elements are also used to model the ballast mass and the non-structural elements such as safeguards and edge beams of the deck. Special focus is given to the track modelling, since it may strongly influence the behaviour of the vehicle. Regarding the vehicle, it consists of a Japanese high-speed train with axle loads of 110 kN whose model was also developed in ANSYS®. Details about these models can be found in [8].

3.2. Seismic action

The seismic excitations adopted in the present study consist of artificial accelerograms generated from the elastic spectra described in EN 1998-1 [26], with PGA corresponding to moderate events with return periods less than 475 years, which is the reference return period of the design seismic action associated with the no-collapse requirement. Thus, four levels of seismic intensity with return periods of 95 (proposed

return period for the damage limitation requirement of [26]), 150, 225 and 310 years are considered, being the ground motion imposed along the lateral direction.
The artificial accelerograms are generated with the software SeismoArtif [27]. The target elastic spectra have been defined for the seismic zone 2.3 of the Portuguese territory and for a soil type A, with an importance factor of 1.0 (railway bridge). The PGA, provided by National Laboratory for Civil Engineering of Portugal, corresponding to the seismic actions considered in this work are presented in Table 2.

Return period (years)	**95**	**150**	**225**	310
PGA ($m.s^{-2}$)	0.862	1.050	1.250	1.420

Table 2: PGA corresponding to the return periods of the seismic actions.

3.3. Results

To analyse the influence of the seismic intensity in the train's running safety, the maximum values of the safety criteria obtained for each seismic intensity level in a scenario in which the vehicle crosses the viaduct at 350 km/ are presented in Table 3. While the Nadal and Prud'homme criteria, which depend on the *Y/Q* ratio and on the lateral contact force, respectively, are significantly affected by the earthquake, the wheel unloading criterion, which depends exclusively on the vertical contact forces, shows a lesser variation. This is due to the fact that only the lateral component of the earthquake is accounted.

Seismic level	**Unloading**	**Prud'homme**	**Nadal**
No earthquake	0.72	0.37	0.26
T = 95 years	0.76	0.89	0.71
T = 150 years	0.82	1.17	0.70
T = 225 years	0.89	1.35	1.02
T = 310 years	0.89	1.42	1.05

Table 3: Maximum values of the safety criteria for different seismic intensities.

The Nadal and wheel unloading criteria obtained for the left wheel of the second wheelset for the minimum and maximum intensities are plotted in Figure 2. As it can be observed, the Nadal criterion is significantly dependent on the seismic action when the vehicle is over the viaduct, while the wheel unloading criterion is barely affected.

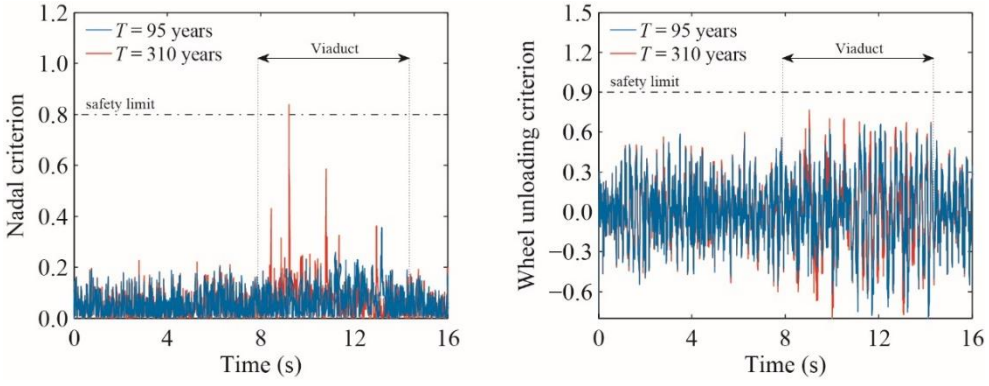

Figure 2: Nadal and unloading criteria for the left wheel of the 2nd wheelset in a scenario with V = 350 km/h

To evaluate the influence of train's speed in its safety, the maximum values of the running safety criteria obtained for vehicle speeds ranging from 200 km/h to 350 km/h in a scenario with an earthquake action with a return period of 150 years are shown in Table 4. The vehicle speed has an important influence in both the vertical and the lateral dynamics.

Speed (km/h)	Unloading	Prud'homme	Nadal
200	0.88	0.90	0.75
250	0.89	0.95	0.82
300	0.90	0.97	0.95
350	1.00	1.68	2.64

Table 4: Maximum values of the safety criteria for different running speeds.

Figure 3 shows the Nadal and wheel unloading criteria obtained for the left wheel of the first wheelset when the vehicle is running at 200 km/h and 350 km/h. Both the lateral and the vertical dynamics are affected by the running speed of the vehicle.

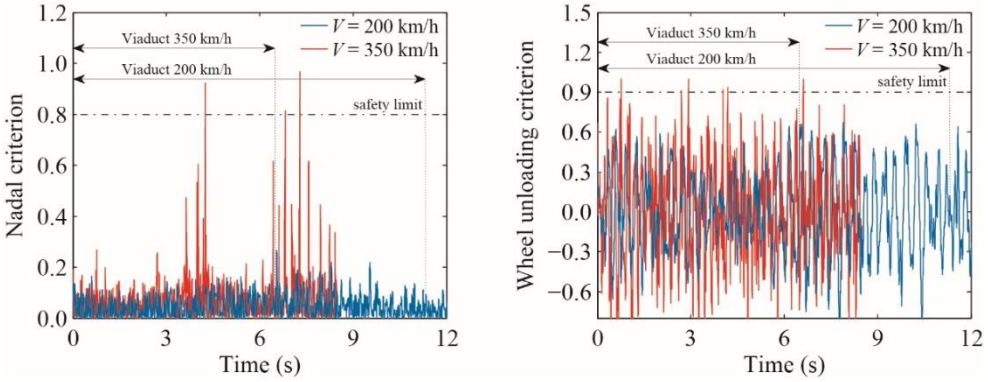

Figure 3: Nadal and unloading criteria for the left wheel of the first wheelset in a scenario with an earthquake with T = 150 years.

The global envelope of each of the analysed safety criterion, as function of the running speed of the vehicle and of the seismic intensity, calculated for the alert limit level of irregularities, is plotted in Figure 4. Each point corresponds to the maximum seismic intensity that guarantees the safety of the vehicle for each running speed. As expected, the tendency observed in all the criteria is similar, indicating that the risk of derailment increases with the increasing of the speed and seismic intensity.

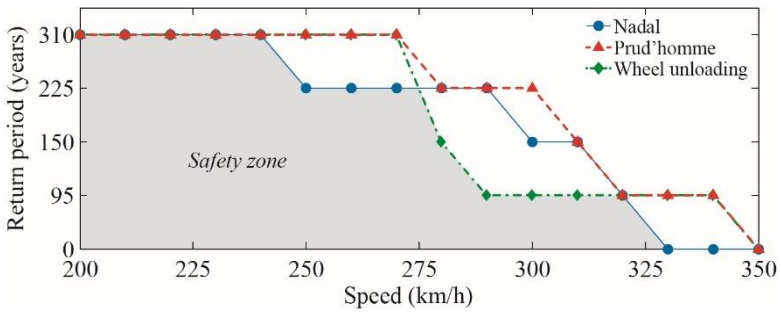

Figure 4: Running safety chart obtained for the alert limit level of irregularities.

4 Case study – running safety against crosswinds

4.1. Case study presentation

The case study adopted in this work is the Arroyo de Las Piedras viaduct located in the Córdoba-Málaga HS line in Spain. It consists of a double track steel-concrete composite deck with 19 continuous spans of 50.4 + 17 × 63.5 + 44 + 35 m. Its cross-section is 6.00 m wide and is formed by two 3.85 m high steel girders and a 0.41 m thick top reinforced concrete slab. To avoid distortion of the deck, K-shape diaphragms are located every 8 m, while a 0.14 m thick prefabricated slab is installed in the bottom to close the torsional flow. A cast-in-place concrete bottom slab is added in the negative moments locations above the columns to increase the longitudinal and torsional stiffness in these areas (double composite action deck).

The vehicle used in this work consists of a Siemens Velaro AVE-S103 with axle loads of approximately 15.5 t. The numerical models of the vehicle and bridge are described in detail in [13]. To evaluate the influence of the bridge dynamic response in the train's safety and passenger comfort, a parametrization the viaduct has been considered to allow different lateral flexibilities. Since the original viaduct has considerably high and slender piers, it is used in this work as the base scenario to represent structures with high flexibility. By modifying the pier properties, it was possible to add three more scenarios, namely two with lower flexibilities and one with higher. Thus, for a certain scenario i, the relative flexibility $\Delta\delta_i$ of the corresponding model is defined in relation to the flexibility of the original viaduct by

$$\Delta\delta_i = \frac{\delta_i}{\delta_0} \tag{3}$$

where δ_i and δ_0 are the lateral flexibilities of the structural models from scenario i and original viaduct, i.e. the displacement at the deck's midpoint caused by a unit lateral load applied in that same point. The four scenarios are presented in Table 5, in which the scenario *S1* represents purely rigid structure (only the track flexibility is considered), scenario *S3* represents the original viaduct and scenarios *S2* and *S4* represent a model with higher and lower piers' stiffness, respectively.

Scenario *i*	**Description**	**Relative flexibility $\Delta\delta_i$ (%)**
S1	Rigid viaduct	0
S2	Medium flexibility	50
S3	Original viaduct (high flexibility)	100
S4	Very high flexibility	150

Table 5: Scenarios that define the viaducts' models based on their lateral flexibility.

4.2. Wind action

The wind velocity field has been generated through the procedure proposed by Cao et al. [28] especially developed for bridges. The drag $F_{d,j}$ and lift $F_{l,j}$ wind loads per unit length applied to the bridge (see Figure 5a) at each generation point *j* are given by

$$F_{d,j}(t) = \frac{1}{2}\rho\, V_j(t)^2\, C_{d,j}(\alpha)\, H_j \tag{4}$$

$$F_{l,j}(t) = \frac{1}{2}\rho\, V_j(t)^2\, C_{l,j}(\alpha)\, B_j \tag{5}$$

where $C_{d,j}(\alpha)$ and $C_{l,j}(\alpha)$ are the drag and lift aerodynamic coefficients, respectively, at the generation point j, α is the wind incidence angle, H_j and B_j are the height and width of the wind exposed area at point j, ρ is the air density and V_j is the resultant wind velocity in *j*.

The total aerodynamic force applied to the vehicle (see Figure 5b) i expressed as

$$F_{f,v}(t) = \frac{1}{2}\rho\, A\, C_{f,v}(\beta)\, V_r(t)^2 \tag{6}$$

where *A* is the reference area, $C_{f,v}(\beta)$ is a generic aerodynamic coefficient (drag, *f=d*, or lift, *f=l*), which is function of the yaw angle β, and $V_r(t)$ is the relative velocity between the wind and vehicle also expressed in detail in [29]. After several mathematical manipulations, it is possible to separate total force into the mean and fluctuating components and applied them to the vehicle during the dynamic analysis.

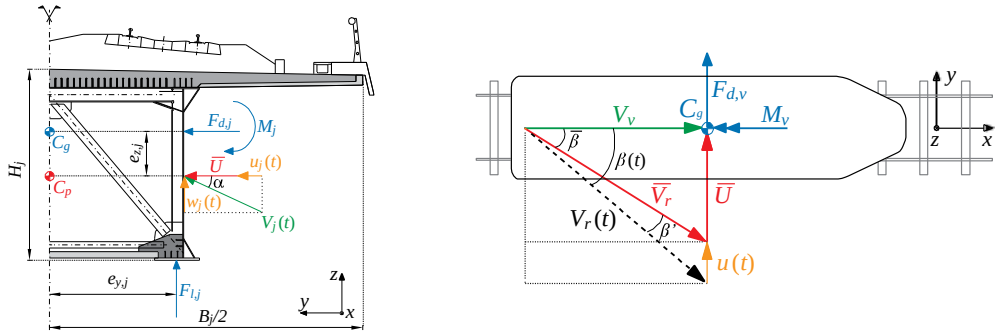

(a) (b)

Figure 5: Wind aerodynamic forces applied to the (a) bridge and (b) vehicle

4.3. Results

To evaluate how the lateral flexibility of the viaduct influences the viaduct response, Figure 6 illustrates the critical train speeds for the different derailment indexes and for the four flexibility scenarios presented in Section 4.1. Contrary to what may be expected, the train's performance in the different scenarios is practically the same, showing the viaduct's lateral dynamic behaviour has a low impact in the traffic safety. Such phenomenon may be explained by the fact that the wind acting on the bridge causes only a smooth and low frequency lateral movement to the deck, and consequently to the track, allowing the train to easily follow it due to the friction forces acting on the wheel-rail interface. This low-frequency lateral movement of the bridge is, therefore, insufficient to impose a sudden and aggressive response to the train. This is a very interesting conclusion, since it may allow significant simplifications in the structural models when the sole objective of the analysis is to study the train running safety against crosswinds. Another important conclusion is related to the most critical derailment index. It can be observed that the Nadal criterion is not determinant, while the unloading and Prud'homme criteria defined the safety boundary for lower and

higher train speeds, respectively. Such result may be explained by the fact that, for higher speeds, the high frequency impacts between wheel and rail due to the track irregularities become more pronounced, leading to higher lateral contact forces, while the unloading phenomenon continues to be mostly controlled by the wind and associated to lower frequency movements of the carbody.

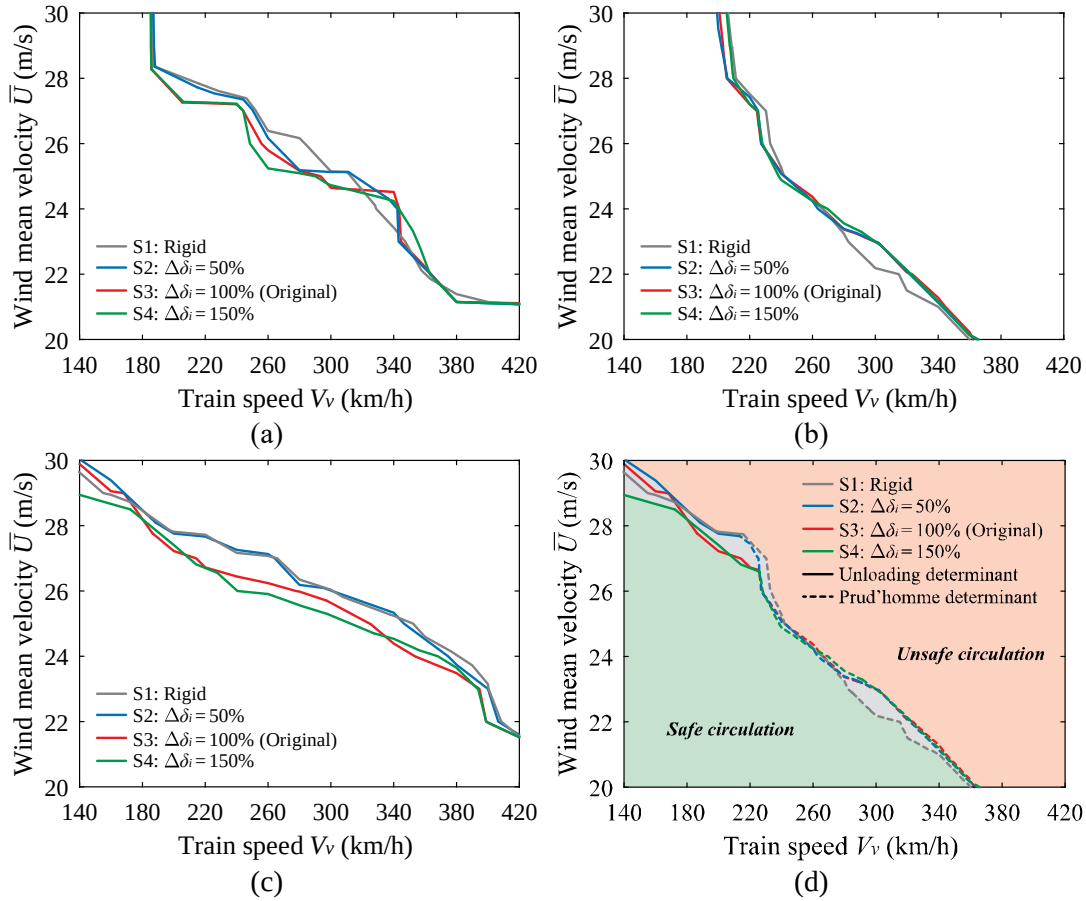

Figure 6: Running safety charts for the four flexibility scenarios relative to the (a) Nadal, (b) Prud'homme and (c) unloading indexes and to the (d) intersection between them.

5 Ongoing and future research

With the methodologies to explicitly analyse the train running safety on bridges already matured through TTBI modelling, it is important to define the future research in this field. The present section briefly describes the ongoing work by the author's research team in the University of Porto (UPORTO) in the field of train safety.

5.1. New perspectives of the deck acceleration criterion in ballasted track bridges

On the subject of the applied criteria for traffic safety, one of the conditions stated in EN 1990-Annex A2 [16] is that vertical deck acceleration must be limited to 3.5 m/s^2 on ballasted track bridges. This criterion comes from the experimental campaigns, held at the German Federal Institute for Materials Research and Training (BAM),

concerned a ballasted track (simulated by a 3 m steel box filled with ballast and four embedded sleepers connected by rails) subjected to varying vertical accelerations. These tests confirmed a previous investigation by the SNCF demonstrating that the ballast layer loses its interlocking capabilities when it experiences accelerations upwards of 0.7g [30]. The fact that EN 1990-Annex A2 [16] then provides a limit of 0.35 g for ballasted tracks is indicative of a safety factor of 2.0. This partial safety factor γ_{bf} is defined as:

$$\gamma_{bf} = \frac{a_{Rk}}{a_{Ed}} \tag{7}$$

where a_{Rk} is the experimentally or normative defined limit (7 m/s^2 for ballasted tracks) and a_{Ed} is the maximum midspan vertical deck acceleration calculated in the design phase at a critical speed defined as the lowest speed corresponding to a specified probability of failure p_f. Since whether dealing with track instability or derailment the target probabilities of failure are very low (in the order of 10^{-4}), typical Monte Carlo trials demand a great deal of computation cost. Work is being carried out, therefore, using Subset Simulation techniques to mitigate this issue. Preliminary calculations using bridge models with different spans subjected to the passage of the HSLM specified in EN 1991-2 [17] point to partial safety factors γ_{bf} lower than 2.0, leading a higher normative deck acceleration limit and, consequently, reduction in the bridge costs without jeopardizing the traffic safety.

5.2. New perspectives of the deck acceleration criterion in non-ballasted track bridges

The assessment of running safety of non-ballasted track bridges is conditioned by the EN 1990-Annex A2 [16] by limiting vertical deck acceleration to 5 m/s^2. The background for this value is not clear, and it is believed that it originates in the application of an arbitrary safety factor of 2 on accelerations around 1 g to avoid loss of wheel–rail contact. However, this relation is not supported by numerical simulations or experimental data, which represents an important gap in the current codes. Therefore, the European project InBridge4EU [31] aims to revise this criterion by analysing its validity through TTBI analysis. Preliminary results have been recently published by Ferreira et al. [32] that showing that for situations were the deck acceleration limit is exceeded, the values of the unloading and Nadal criteria are still well below the limit value. Such results prove that the empirical relationship between deck acceleration and actual derailment is not adjusted.

5.3. New developments in the TTBI models for train running safety analysis

TTBI analysis have a very high computation demand, but indispensable for the assessment of the risk o derailment of train moving over bridges. To overcome this issue and to allow the development of probabilistic analysis of train running safety through TTBI models, an AI methodology for predicting wheel-rail contact forces will be developed in the future to save computational time and reduce the number of necessary dynamic analysis. Hybrid algorithms have been shown to increase computational efficiency and are an emerging topic that can be explored in order to enable probabilistic analyses (zhang˙efficient˙2023; WANG; ZHANG; HAN et al., 2024).

6 Conclusions

The present paper presents a TTBI methodology for analysing risk of derailment of trains moving over bridges. After presenting this model, two case studies are discussed: one related with safety against earthquakes and a second one against crosswinds.

For the first case study, special attention is given to moderate earthquakes, which, although do not pose a significant threat to the structure, they may jeopardize the stability of the vehicle and, consequently, to the safety of the passengers. The results shown that, even for the moderate seismic intensities considered in the present study, the train safety is put at risk in a considerable number of scenarios. These results prove the importance of taking low intensity earthquakes into account in the design of railway bridges.

Regarding the second case study, the results shown that, although different structural bridge configurations lead to distinct dynamic responses, it does not affect the vehicle's performance in terms of running safety. Such phenomenon may be explained by the fact that the wind acting on the bridge causes only a smooth and low frequency lateral movement to the deck, and consequently to the track, allowing the train to easily follow it due to the friction forces acting on the wheel-rail interface.

Finally, some topics related to ongoing and future work in the area of train running safety were briefly presented, namely the enhancement currently being carried out in European projects of the traffic safety criteria stipulated in the EN1990-A2, such as the deck acceleration or the deck deformation limits.

Acknowledgements

The authors would like also to acknowledge the financial support of the project InBridge4EU funded by the Europe's Rail Joint Undertaking under Horizon Europe research and innovation programme under grant agreement No. 101121765 (HORIZON-ER-JU-2022-ExplR-02). This work was also financially supported by: Base Funding - UIDB/04708/2020 with DOI 10.54499/UIDB/04708/2020 (https://doi.org/10.54499/UIDB/04708/2020) and Programmatic Funding - UIDP/04708/2020 with DOI 10.54499/UIDP/04708/2020 (https://doi.org/10.54499/UIDP/04708/2020) of the CONSTRUCT - Instituto de I&D em Estruturas e Construções - funded by national funds through the FCT/MCTES (PIDDAC) and Grant no. 2022.00628.CEECIND from the Stimulus of Scientific Employment, Individual Support (CEECIND) – 5th Edition provided by ''FCT – Fundação para a Ciência e Tecnologia''.

References

[1] Montenegro, P. A., Carvalho, H., Ribeiro, D., Calçada, R., Tokunaga, T., Tanabe, M., & Zhai, W. (2021). Assessment of train running safety on bridges: A literature review. *Engineering Structures, 241*, 112425.

[2] Arvidsson, T., Andersson, A., & Karoumi, R. (2019). Train running safety on non-ballasted bridges. *International Journal of Rail Transportation, 7*(1), 1-22.

[3] Ling, L., Dhanasekar, M., & Thambiratnam, D. P. (2018). Dynamic response of the train–track–bridge system subjected to derailment impacts. *Vehicle System Dynamics, 56*(4), 638-657.

[4] Xia, C. Y., Xia, H., & De Roeck, G. (2014). Dynamic response of a train–bridge system under collision loads and running safety evaluation of high-speed trains. *Computers & Structures, 140*, 23-38.

[5] Chen, Z., & Zhai, W. M. (2020). Theoretical method of determining pier settlement limit value for China's high-speed railway bridges considering complete factors. *Engineering Structures, 209*, 109998: 109991-109912. DOI:10.1016/j.engstruct.2019.109998

[6] Han, Z., Chen, Z., & Zhai, W. M. (2018). Effect of wheel polygonal wear on dynamic responses of high speed train-track-bridge system. In M. Spiryagin, T. Gordon, C. Cole, & T. McSweeney (Eds.), *Dynamics of Vehicles on Roads and Tracks* (pp. 823-828). London, UK: Taylor & Francis Group.

[7] Tanabe, M., Sogabe, M., Wakui, H., Matsumoto, N., & Tanabe, Y. (2016). Exact Time Integration for Dynamic Interaction of High-Speed Train and Railway Structure Including Derailment During an Earthquake. *Journal of Computational and Nonlinear Dynamics, 11*(3), 031004: 031001:031009.

[8] Montenegro, P. A., Calçada, R., Vila-Pouca, N., & Tanabe, M. (2016). Running safety assessment of trains moving over bridges subjected to moderate earthquakes. *Earthquake Engineering & Structural Dynamics, 45*, 483–504.

[9] Zeng, Q., & Dimitrakopoulos, E. G. (2018). Vehicle–bridge interaction analysis modeling derailment during earthquakes. *Nonlinear Dynamics, 93*, 2315–2337. DOI:10.1007/s11071-018-4327-6

[10] Zhai, W. M., Yang, J., Li, Z., & Han, H. (2015). Dynamics of high-speed train in crosswinds based on an air-train-track interaction model. *Wind and Structures, 20*(2), 143-168.

[11] Antolín, P. (2013). *Efectos dinámicos laterales en vehículos y puentes ferroviarios sometidos a la acción de vientos transversales.* (PhD Thesis), Universidad Politécnica de Madrid, Madrid, Spain.

[12] Montenegro, P. A., Barbosa, D., Carvalho, H., & Calçada, R. (2020). Dynamic effects on a train-bridge system caused by stochastically generated turbulent wind fields. *Engineering Structures, 211*, 110430. DOI:10.1016/j.engstruct.2020.110430

[13] Montenegro, P. A., Carvalho, H., Ortega, M., Millanes, F., Goicolea, J. M., Zhai, W. M., & Calçada, R. (2022). Impact of the train-track-bridge-wind system characteristics in the runnability of high-speed trains against crosswinds - Part I: running safety. *Journal of Wind Engineering and Industrial Aerodynamics, 224*, 104974.

[14] Liu, M., Wang, J., Zhu, H., Krajnovic, S., & Gao, G. (2019). A numerical study of snow accumulation on the bogies of high-speed trains based on coupling improved delayed detached eddy simulation and discrete phase model. *Proceedings of the Institution of Mechanical Engineers, Part F: Journal of Rail and Rapid Transit, 233*(7), 1-16. DOI:10.1177/0954409718805817

[15] RTRI (2006). *Outline of design standards for railway structures and commentary (displacement limits),* Railway Technical Research Institute (Ed.), Maruzen Co., Ltd. Tokyo.
[16] EN 1990-Annex A2 (2009). *Eurocode 0: Basis of structural design - Annex 2: Application for bridges (normative),* European Committee for Standarization (CEN). Brussels.
[17] EN 1991-2 (2017). *Eurocode 1: Actions on structures - Part 2: Traffic loads on bridges,* European Committee for Standarization (CEN). Brussels.
[18] Zhai, W. M., Han, Z., Chen, Z., Ling, L., & Zhu, S. (2019). Train–track–bridge dynamic interaction: a state-of-the-art review. *Vehicle System Dynamics, 57*(7), 984-1027. DOI:10.1080/00423114.2019.1605085
[19] Montenegro, P. A., & Calçada, R. (2023). Wheel–rail contact model for railway vehicle–structure interaction applications: development and validation. *Railway Engineering Science, 31*(3), 181–206.
[20] Montenegro, P. A., Neves, S. G. M., Calçada, R., Tanabe, M., & Sogabe, M. (2015). Wheel-rail contact formulation for analyzing the lateral train-structure dynamic interaction. *Computers & Structures, 152*, 200-214.
[21] Neves, S. G. M., Montenegro, P. A., Azevedo, A. F. M., & Calçada, R. (2014). A direct method for analyzing the nonlinear vehicle–structure interaction. *Engineering Structures, 69*, 83-89.
[22] Kalker, J. J. (1996). *Book of tables for the Hertzian creep-force law*.*Presented in* 2nd Mini Conference on Contact Mechanics and Wear of Wheel/Rail Systems, Budapest, Hungary
[23] EN 14363 (2016). *Railway applications - Testing and Simulation for the acceptance of running characteristics of railway vehicles - Running Behaviour and stationary tests,* European Committee for Standarization (CEN). Brussels.
[24] EN 14067-6 (2016). *Railway applications - Aerodynamics - Part 6: Requirements and test procedures for cross wind assessment,* CEN. Brussels.
[25] ANSYS®. (2018). Canonsburg, PA, USA: Academic Research, Release 19.2, ANSYS Inc.
[26] EN 1998-1 (2004). *Eurocode 8: Design of structures for earthquake resistance - Part 1: General rules, seismic actions and rules for buildings,* European Committee for Standarization (CEN). Brussels.
[27] SeismoArtif. (2013). Pavia, Italy: Version 2.1, SeismoSoft.
[28] Cao, Y., Xiang, H., & Zhou, Y. (2000). Simulation of Stochastic Wind Velocity Field on Long-Span Bridges. *Journal of Engineering Mechanics, 126*(1), 1-6.
[29] Montenegro, P. A., Heleno, R., Carvalho, H., Calçada, R., & Baker, C. J. (2020). A comparative study on the running safety of trains subjected to crosswinds simulated with different wind models. *Journal of Wind Engineering and Industrial Aerodynamics, 207*, 104398.
[30] Zacher, M., & Baeßler, M. (2008). Dynamic behaviour of ballast on railway bridges. In R. Delgado, R. Calcada, J. M. Goicolea, & F. Gabaldon (Eds.), *Dynamics of High-Speed Railway Bridges* (pp. 125-142). London, UK: CRC Press.

[31] InBridge4EU (2023). Enhanced Interfaces and train categories FOR dynamic compatibility assessment of European railway BRIDGEs. Retrieved from https://inbridge4eu.eu/project/

[32] Ferreira, G., Montenegro, P. A., Andersson, A., Henriques, A. A., Karoumi, R., & Calçada, R. (2024). Critical analysis of the current Eurocode deck acceleration limit for evaluating running safety in ballastless railway bridges. *Engineering Structures*, *312*, 118127.